

SHORT COMMUNICATION

First Application of Whole Genome Sequencing in Myelinated Retinal Nerve Fibers (MRNF)

E. Scott SILLS^{1,2}, Conor HARRITY³, Howard I. CHU⁴, Jing-Wen WANG⁵, Samuel H. WOOD⁵, Seang Lin TAN^{6,7}

¹Center for Advanced Genetics, Regenerative Biology Group, San Clemente, USA, ²Experimental Science Systems, Harriman, USA, ³Department of Obstetrics & Gynaecology, Royal College of Surgeons in Ireland, Dublin, Ireland, ⁴Department of Psychobiology, University of California-Los Angeles; Los Angeles, USA, ⁵Gen 5 Fertility Center, San Diego, USA, ⁶OriginElle Fertility Clinic, Montréal, Canada, ⁷Department of Obstetrics & Gynecology, McGill University, Montréal, Canada

Received December 15, 2023

Accepted January 23, 2024

Summary

Genetic features are currently unknown in myelinated retinal nerve fibers (MRNF). For a 20-year-old asymptomatic female with unilateral MRNF, we performed whole genome sequencing (WGS) by standard workflow protocol to produce contiguous long-read sequences with Illumina DNA PCR-Free Prep. After tagmentation, libraries were sequenced on separate runs via NovaSeq 6000 platform at 2 x 150bp read length. Gene variants included rs2248799, rs2672589, rs7555070, rs247616_T and rs2043085_C all associated with an increased macular degeneration risk, and seven novel variants of uncertain significance. For optic disc enlargement, variants rs9988687_A, rs11079419_T, rs6787363 and rs10862708_A suggested an increased risk for this condition. In contrast, modeling revealed retinal detachment risk was reduced by variants identified at rs9651980_T, rs4373767_T, and rs7940691_T which were among five other previously unreported variants. WGS data placed proband at the 66th and 64th percentiles for disc anomaly and retinal detachment risk, respectively. Additionally, risk determined from 16 loci associated with age-related macular degeneration found the patient to be at the 18th percentile for this diagnosis (*i.e.*, below average genetic predisposition). Fundoscopic findings showed mean RNFL thickness was lower with MRNF (77 OS vs. 96µm OD) and RNFL symmetry was impaired (43 %) but stable between 2020 and 2023. Rim area and cup volume were also substantially different (2.33 OS vs. 1.34mm² OD, and 0.001 OS vs. 0.151mm³ OD, respectively). As the first known evaluation of MRNF via WGS, these data reveal a mixed picture with variants associated with different risks for potentially related ocular pathologies. In addition, we identify multiple new variants of unknown

significance. Factors affecting gene expression in MRNF require further study.

Key words

Whole genome sequencing • Retina • Myelination • Anatomy • Gene variants

Corresponding author

E. Scott Sills, P.O. Box 73910, San Clemente, CA 92673 USA.
E-mail: ess@prp.md

Myelinated retinal nerve fibers (MRNF) describe retinal nerve fibers anterior to the lamina cribrosa which retain a myelin sheath, an event noted in about 1 % of patients. It is often diagnosed incidentally with few clinical complaints. First described in 1856 by Virchow, the condition appears as sharply circumscribed gray-white retinal patches [1]. Its etiology remains not known. The finding is often present at birth as a nonprogressive lesion, and familial cases of MRNF have been reported. Here we describe genetic features in the setting of asymptomatic non-progressive unilateral MRNF, believed to be the first application of whole genome sequencing (WGS) for this condition.

Clinical presentation: A 20-year-old female attended for follow-up ophthalmic examination. The patient was a well-adjusted college student with BMI = 17.5. She did not use eye drops or tobacco and her surgical

history was negative. Her medical history was notable for being a known carrier of three gene variants at *RUNX2*, *SALL1*, and *SAMD9*, with ophthalmology referral and WGS included in her post-hospitalization care plan after COVID-19. She had been diagnosed with strabismus during early pediatric checks, and corrective lenses at age 18mo were revised at periodic exams. By high school graduation, glasses were no longer needed. At the most recent exam there were no field defects and acuity by Snellen was 20/30, bilaterally. Unilateral (left) MRNF was serially monitored with no changes recorded over 10 years. Her only daily medications were oral contraceptives and 2.5mg enalapril, the latter prescribed for intermittent proteinuria. When increased urine protein and fluctuating glomerular filtration rate emerged in 2023, an unscheduled eye evaluation was recommended before proceeding to renal biopsy.

Assessment included optical coherence tomography (macula & anterior segment), ONA/optic nerve, endothelial cell count, amplitude scan, bright scan ultrasound, fluorescein & ICG angiography, pachymetry, slit-lamp exam, color perception, refraction and visual field mapping. Retinal nerve fiber layer (RNFL) thickness was notably reduced with MRNF (77 OS vs. 96 μ m OD), and RNFL symmetry was low (43 %) but unchanged between 2020 and 2023. Rim area and cup volume in 2023 were substantially different (2.33 OS vs. 1.34mm² OD, and 0.001 OS vs. 0.151mm³ OD, respectively).

WGS data were collected using standard workflow to produce contiguous long-read sequences on

the NovaSeqTM 6000 System and NovaSeq X Series [2]. Briefly, long DNA fragments were enzymatically indexed with landmarks. Unmarked libraries to produce contiguous long reads for the original single-molecule fragment were prepared using Illumina DNA PCR-Free Prep, Tagmentation (Illumina cat.# 20041794). Libraries were then sequenced on separate runs via NovaSeq 6000 System at 2 x 150bp read length. Because current experience has yet to correlate specific variants with MRNF, this investigation cross-referenced regions with known association with retinal structure or function based on reported variants associated with optic disc morphology, retinal detachment, and age-related macular degeneration.

Reference metrics of optic disc morphology were derived from 115 genetic variants associated with optic disc size and vertical cup-to-disc ratio [3]. From such reports, proband data were calculated at the 66th percentile (*i.e.*, above average genetic predisposition to disc enlargement). For retinal detachment 11 genetic variants associated with this condition were considered [4], and the proband was placed at the 64th percentile consistent with above average genetic predisposition to retinal detachment. However, macular degeneration risk based on 16 loci associated with age-related macular degeneration [5] placed the proband at the 18th percentile (*i.e.*, below average genetic predisposition). Variants sufficiently rare or new were provisionally classified under macular degeneration ($n=7$), optic disc enlargement ($n=59$), and retinal detachment ($n=8$) as shown in Table 1a and 1b.

Table 1a. Leading variants identified in unilateral MRNF via whole genome sequencing (WGS) with reference to age-related macular degeneration, optic disc size anomalies, and retinal detachment vs. a WGS private library ($n=5,000$) ranked by effect size. Imputed polygenic scores (+/-) estimated proband's relative risk for each disorder.

| | variant | CR | PG | effect size | VAF (%) |
|---------------------------------|--------------|-------------|-----|-------------|----------|
| <i>macular degeneration (-)</i> | rs2248799 | 10q26 | C/T | 0.61 | 49 |
| | rs2672589 | 10p14 | A/A | 0.47 | 61 |
| | rs7555070 | 1p13 | T/T | 0.46 | 68 |
| | rs247616_T | 16q13 | C/T | 0.17 | 33 |
| | rs2043085_C | 15q21 | C/C | 0.14 | 61 |
| <i>optic disc (+)</i> | rs9988687_A | 10p13 | A/A | 0.07 | 77 |
| | rs6787363 | 3p13 | A/A | 0.02 | 38 |
| | rs10862708_A | 12p13/12q21 | A/A | 0.02 | 56 |
| <i>retinal detachment (+)</i> | rs9651980_T | 12p14 | T/T | 0.17 | 9 |
| | rs4373767_T | 1p14 | C/T | 0.12 | 63 |
| | rs7940691_T | 11p13 | C/T | 0.11 | 36 |

Notes: CR=cytogenetic region, PG=proband genotype, VAF=variant allele frequency. For all entries, $p<0.0001$.

Table 1b. Previously unknown or new variants identified in unilateral MRNF via whole genome sequencing (WGS) with reference to reports associated with age-related macular degeneration ($n=69$), optic disc size anomalies ($n=115$), and retinal detachment ($n=11$).

| | variant | PG | effect size | VAf (%) |
|-----------------------------|--------------|-------|-------------|---------|
| <i>macular degeneration</i> | rs3825991_A | C/A | 0.09 | 48 |
| | rs1926564_A | A/A | -0.14 | 90 |
| | rs1378940_A | C/A | 0.09 | 68 |
| | rs259842_C | C/C | -0.08 | 62 |
| | rs11120691_G | G/G | -0.08 | 44 |
| | rs1005819_T | C/T | -0.08 | 42 |
| | rs17421419_G | A/G | 0.15 | 7 |
| <i>optic disc</i> | rs11079419_T | T/C | 0.03 | 20 |
| | rs9905786_T | T/T | 0.02 | 64 |
| | rs4839470_T | C/T | -0.02 | 24 |
| | rs12436074_A | A/A | -0.02 | 56 |
| | rs73173591_A | T/A | 0.03 | 9 |
| | rs72759609_T | T/T | 0.03 | 90 |
| | rs76567987_A | A/A | 0.02 | 84 |
| | rs3857971_A | G/A | -0.02 | 30 |
| | rs74056359_A | A/A | -0.02 | 83 |
| | rs7744813_A | C/A | -0.02 | 59 |
| | rs61975075_A | A/A | 0.03 | 94 |
| | rs9330799_A | A/A | -0.02 | 53 |
| | rs2092524_A | G/A | 0.01 | 34 |
| | rs9967780_T | G/T | 0.02 | 22 |
| | rs906568_T | T/T | -0.01 | 36 |
| | rs1905014_T | T/T | -0.01 | 57 |
| | rs1550094_A | G/A | 0.01 | 69 |
| | rs10764494_A | C/A | 0.01 | 68 |
| | rs35285683_A | A/A | -0.02 | 85 |
| | rs7717697_T | T/T | 0.01 | 59 |
| | rs11564398_T | T/T | 0.01 | 72 |
| | rs7188859_T | T/C | 0.01 | 63 |
| | rs72784719_A | A/A | 0.06 | 99 |
| | rs77877421_A | A/A | -0.03 | 94 |
| | rs698153_A | A/A | -0.03 | 95 |
| | rs71296770_A | A/A | -0.02 | 90 |
| | rs6673575_A | G/A | 0.01 | 32 |
| | rs2033054_T | C/T | -0.01 | 65 |
| | rs10957177_A | A/G | 0.01 | 75 |
| | rs11584075_A | A/A | 0.02 | 92 |
| | rs10164395_T | C/T | -0.01 | 33 |
| | rs6999835_T | T/C | 0.01 | 63 |
| | rs11734073_A | A/A | -0.02 | 87 |
| rs251526_A | A/G | -0.02 | 92 | |
| rs2149108_T | C/T | -0.01 | 40 | |
| rs13417287_T | T/T | -0.01 | 77 | |
| rs2761882_T | C/T | -0.01 | 50 | |

| | | | | |
|---------------------------|--------------|-------|-------|----|
| rs12619508_A | C/A | -0.01 | 47 | |
| rs3754442_T | C/T | 0.01 | 59 | |
| rs59199978_A | A/A | -0.01 | 82 | |
| rs11627052_A | G/A | 0.01 | 22 | |
| rs13022913_T | T/T | -0.01 | 57 | |
| rs78977588_A | C/A | 0.02 | 12 | |
| rs10823610_A | C/A | 0.01 | 56 | |
| rs599892_C | C/C | 0.01 | 70 | |
| rs1852148_A | A/G | -0.01 | 47 | |
| rs10910_T | T/T | 0.01 | 69 | |
| rs6860726_C | G/C | -0.01 | 49 | |
| rs7620608_T | T/T | -0.01 | 61 | |
| rs7615960_A | A/T | -0.02 | 93 | |
| rs2266963_C | C/C | -0.01 | 81 | |
| rs28840750_T | T/G | -0.03 | 96 | |
| rs2430356_A | A/T | -0.01 | 77 | |
| rs11684168_T | T/T | 0.01 | 83 | |
| rs8076249_T | T/T | -0.01 | 60 | |
| rs1901440_A | C/A | -0.01 | 66 | |
| rs30371_T | T/T | -0.01 | 63 | |
| rs28603236_A | A/A | 0.01 | 85 | |
| rs13264644_A | A/G | -0.01 | 57 | |
| <hr/> | | | | |
| <i>retinal detachment</i> | rs74764079_T | T/T | -0.33 | 97 |
| | rs4373767_T | C/T | 0.12 | 63 |
| | rs11187838_G | G/A | -0.11 | 57 |
| | rs1248634_G | G/G | -0.12 | 71 |
| | rs11217712_T | T/T | -0.11 | 31 |
| | rs4243042_T | A/T | -0.12 | 47 |
| | rs7940691_T | C/T | 0.11 | 36 |
| | rs9651980_T | T/T | 0.17 | 9 |

Notes: PG=proband genotype, VAF=variant allele frequency. Negative effect size indicates reduced risk. Retinal detachment variants appear in both tables because all variants were new/unreported. For all entries, $p < 0.0001$.

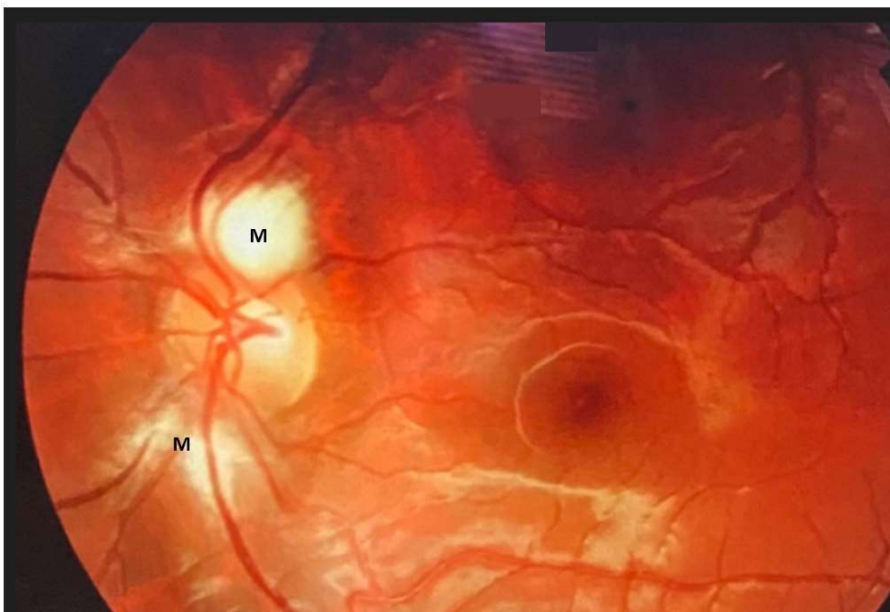


Fig. 1. Fundoscopic findings (left) documenting myelinated retinal nerve fibers (M) at the 2023 exam.

Prior exon sequencing [6] identified variants Q253H in *SALL1* and R824Q in *SAMD9* plus a previously unreported multiexon 3' terminal duplication of *RUNX2*. Since retinal evaluation was reassuring with no vascular changes (Fig. 1), her kidney findings were attributed to a local manifestation of 'long Covid' as an isolated renal process.

For WGS, effect size was defined as contribution of the SNP/mutation to trait genetic variance (gv) = $2\beta^2f(1-f)$ where f is allele frequency for either of two alleles and β is coefficient for a SNP when outcome is modeled by regression [7].

Discussion: MRNFs are caused by presence of ectopic oligodendrocyte-like cells in the retina, leading to myelination of retinal ganglion cell fibers. It occurs when the protective lamina cribrosa barrier is underdeveloped, allowing encroachment of oligodendrocytes into retina. Visual pathway myelination is evident by the 8th gestational month and reaches the posterior globe near term, with most fibers attaining full myelination by age seven months [8]. Myelination usually stops at this stage, but when it progresses beyond the lamina cribrosa, MRNFs are the result [9,10]. The impact of MRNF on visual functioning is variable and likely depends on degree of myelination or macula involvement.

While this project does contribute original WGS data to the understanding of MRNF, there are important constraints on our research. First, WGS sampling was not performed on relatives to construct an informative pedigree. Additionally, MRNF is joined here by exon variants involving *RUNX2*, *SALL1* and *SAMD9*, making generalization to a standard background population difficult. Indeed, these variants draw notice to their potential relevance in the emergence of MRNF independent of information supplied by WGS, particularly as axonal myelination is organized by oligodendrocyte progenitors which migrate via neuroendocrine signaling [8]. Although *RUNX2* has not yet been implicated in MRNF, this is a highly-conserved gene known to regulate ocular development [11], and the protein product *RUNX2* guides transcriptional programs and eye morphogenesis. *RUNX2* also influences

extracellular matrix receptor interaction pathways related to corneal dystrophy/keratoconus [12] and promotes Müller glial cell activation and maintenance of the blood-retina barrier [13]. Recently, a proteomic study of vitreous samples was referenced against a WGS dataset and discovered a previously unknown *RUNX2* pathway involved in angiogenesis [14]. While *SALL1* disruption is not thought to affect microglial colonization of retina and cortex [15], microglial morphology during retinal development changed from ramified to amoeboid in a murine *SALL1* knockout model [16].

Regarding *SAMD9*, no retinal features have been reported among patients with mutations at this locus or with its associated 'MIRAGE' syndrome (*i.e.*, myelodysplasia, infection, growth restriction, adrenal hypoplasia, genital phenotypes, and enteropathy). Current guidance for eye care with *SAMD9* variants is routine (*i.e.*, artificial tears for hypolacrimation) [17].

Conclusion: This report shares the first WGS data on unilateral asymptomatic MRNF. In our case, MRNF remained stable over many years, despite—or perhaps because of—three gene variants not previously associated with MRNF. As a developmental mechanism for MRNF awaits clarification, it is hoped that increased availability and lower cost of WGS will enable broader knowledge of this unusual condition going forward.

Conflict of Interest

There is no conflict of interest.

Authors' contributions

ESS developed the project; HC, HIC, J-WW, SHW and SLT reviewed the literature and edited revisions. All authors read and approved the final version.

Acknowledgements

Acknowledgements: The authors are grateful to Ms. Lisa A. Balducci for patient coordination and data analysis.

Availability of data and material: Redacted records are available upon written request to the corresponding author.

References

1. Panigrahi A, Singh A, Gupta V. Syndrome of myelinated nerve fibers, hyperopia, strabismus, and amblyopia. *Ophthalmol Retina* 2022;6(12):1153. <https://doi.org/10.1016/j.oret.2022.10.003>
2. Ibrahim I, Scriver T, Basalom SA. No, it is not mutually exclusive! A case report of a girl with two genetic diagnoses: Craniofrontonasal dysplasia and pontocerebellar hypoplasia type 1B. *Clin Case Rep* 2023;11(5):e7332. <https://doi.org/10.1002/ccr3.7332>

3. Han X, Qassim A, An J, Marshall H, Zhou T, Ong JS, et al. Genome-wide association analysis of 95,549 individuals identifies novel loci and genes influencing optic disc morphology. *Hum Mol Genet* 2019;28(21):3680-3690. <https://doi.org/10.1093/hmg/ddz193>
 4. Boutin TS, Charteris DG, Chandra A, Campbell S, Hayward C, Campbell A, et al. Insights into the genetic basis of retinal detachment. *Hum Mol Genet* 2020;29(4):689-702. <https://doi.org/10.1093/hmg/ddz294>
 5. Han X, Gharahkhani P, Mitchell P, Liew G, Hewitt AW, MacGregor S. Genome-wide meta-analysis identifies novel loci associated with age-related macular degeneration. *J Hum Genet* 2020;65(8):657-665. <https://doi.org/10.1038/s10038-020-0750-x>
 6. Sills ES, Wood SH. Phenotype from SAMD9 mutation at 7p21.2 appears attenuated by novel compound heterozygous variants at RUNX2 and SALL1. *Glob Med Genet* 2022;9(2):124-128. <https://doi.org/10.1055/s-0041-1740018>
 7. Park JH, Wacholder S, Gail MH, Peters U, Jacobs KB, Chanock SJ, et al. Estimation of effect size distribution from genome-wide association studies and implications for future discoveries. *Nat Genet* 2010;42(7):570-575. <https://doi.org/10.1038/ng.610>
 8. Magoon EH, Robb RM. Development of myelin in human optic nerve and tract. A light and electron microscopic study. *Arch Ophthalmol* 1981;99(4):655-659. <https://doi.org/10.1001/archoph.1981.03930010655011>
 9. Ffrench-Constant C, Miller RH, Burne JF, Raff MC. Evidence that migratory oligodendrocyte-type-2 astrocyte (O-2A) progenitor cells are kept out of the rat retina by a barrier at the eye-end of the optic nerve. *J Neurocytol* 1988;17(1):13-25. <https://doi.org/10.1007/BF01735374>
 10. Balraj A, Clarkson-Paredes C, Miller RH. Loss of optic nerve oligodendrocytes during maturation alters retinal organization. *Exp Eye Res* 2023;233:109540. <https://doi.org/10.1016/j.exer.2023.109540>
 11. Postlethwait JH, Yan YL, Desvignes T, Allard C, Titus T, Le François NR, et al. Embryogenesis and early skeletogenesis in the antarctic bullhead notothen, *Notothenia coriiceps*. *Dev Dyn* 2016;245(11):1066-1080. <https://doi.org/10.1002/dvdy.24437>
 12. Sun X, Gao X, Mu BK, Wang Y. Understanding the role of corneal biomechanics-associated genetic variants by bioinformatic analyses. *Int Ophthalmol* 2022;42(3):981-988. <https://doi.org/10.1007/s10792-021-02081-9>
 13. Ji N, Guo Y, Liu S, Zhu M, Tu Y, Du J, et al. MEK/ERK/RUNX2 Pathway-mediated IL-11 autocrine promotes activation of Müller glial cells during diabetic retinopathy. *Curr Eye Res* 2022 Dec;47(12):1622-30. <https://doi.org/10.1080/02713683.2022.2129070>
 14. Valdivia AO, He Y, Ren X, Wen D, Dong L, Nazari H, et al. Probable treatment targets for diabetic retinopathy based on an integrated proteomic and genomic analysis. *Transl Vis Sci Technol* 2023;12(2):8. <https://doi.org/10.1167/tvst.12.2.8>
 15. Koso H, Tshako A, Lai CY, Baba Y, Otsu M, Ueno K, et al. Conditional rod photoreceptor ablation reveals Sall1 as a microglial marker and regulator of microglial morphology in the retina. *Glia* 2016;64(11):2005-24. <https://doi.org/10.1002/glia.23038>
 16. Koso H, Nishinakamura R, Watanabe S. Sall1 Regulates Microglial Morphology Cell Autonomously in the Developing Retina. *Adv Exp Med Biol* 2018;1074:209-15. https://doi.org/10.1007/978-3-319-75402-4_26
 17. Tanase-Nakao K, Olson TS, Narumi S. MIRAGE Syndrome. 2020 Nov 25. In: Adam MP, Mirzaa GM, Pagon RA et al (eds). *GeneReviews*. Seattle (WA): University of Washington, Seattle; 1993-2023. <https://www.ncbi.nlm.nih.gov/books/NBK564655/>
-